Polymer Testing 58 (2017) 126–134

Contents lists available at ScienceDirect

Polymer Testing

journal homepage: www.elsevier.com/locate/polytest

Material Performance

Natural superabsorbent plastic materials based on a functionalized soy protein

A.A. Cuadri [a], A. Romero [b], C. Bengoechea [b], A. Guerrero [b, *]

[a] Departamento de Ingeniería Química, Centro de Investigación en Tecnología de Productos y Procesos Químicos (Pro²TecS), Campus de 'El Carmen', Universidad de Huelva, 21071, Huelva, Spain
[b] Departamento de Ingeniería Química, Universidad de Sevilla, Facultad de Química, 41012 Sevilla, Spain

ARTICLE INFO

Article history:
Received 17 November 2016
Accepted 21 December 2016
Available online 24 December 2016

Keywords:
Superabsorbent polymers
Plastics
Water uptake capacity
Succinic anhydride
FTIR
Protein functionalization

ABSTRACT

A natural superabsorbent polymer (SAP) material based on an acylated soy protein was studied as a green alternative to non-biodegradable SAP. In order to obtain the natural SAPs, different amounts of succinic anhydride were used as acylating agent. Once the functionalized protein was obtained, it was mixed thoroughly with glycerol and then molded through a lab-scale injection molding device. Water uptake of samples obtained reached values much higher than those based on unacylated protein. Moreover, a greater extent of the acylation reaction led to higher water uptake values for the corresponding SAPs, probably related to their higher hydrophilic character. Water imbibing capacity measurements and thermogravimetrical analysis (TGA) seemed to confirm this. The presence of larger porous regions in acylated samples observed in SEM images could also play a role in their higher water uptake values.

Furthermore, an increase in the extent of acylation reaction led to plastics with lower Young's modulus and higher extensibility.

1. Introduction

Superabsorbent polymer (SAP) materials are defined as hydrophilic three-dimensional polymer networks that can absorb and retain a significant amount of water or biological fluids (as high as ~ 10–1000 times their own weight) [1–3]. Regarding their applications, the super-swelling characteristics of SAPs makes them ideal materials in engineering, biological and pharmaceutical products [4], highlighting the uses for water retention in agriculture and horticulture soils [5] and, mainly, for disposable diapers and feminine hygiene products [6].

SAPs are generally classified into synthetic and natural-based polymers. The former are frequently produced from acrylic acid and its derivatives [7,8], issues related to their poor biodegradability and high costs having been pointed out [1]. As a consequence, there is a growing need to develop natural SAPs that overcome these drawbacks, showing both great water uptake capacity and processability.

In this sense, some studies have reported the synthesis of bio-based SAP materials prepared from polysaccharides such as cellulose [9], starch [10], carrageenan [11] or gelatin [12]. However, the low efficiency when compared to synthetic SAPs together with the resulting high cost of production are factors that limit the application of polysaccharides-based SAPs [13,14]. On the other hand, the use of proteins might be a promising alternative in the production of natural SAPs, in spite of the relatively moderate water uptake capacity shown by most of them under native conditions. Proteins contain more than 20 different aminoacids [15] characterized by numerous reactive groups that can be used as sites for chemical modifications and cross-linking to develop polymeric structures [16]. In addition to that, proteins may be the most underrated and underutilized feedstocks with respect to their applications [1] and, consequently, their use as natural-based SAP materials would provide substantial added value.

Soy protein would seem to be an adequate starting material for the manufacture of natural-based SAP materials when considering the following facts: (1) it is the main coproduct of the soybean oil industry, being available at an affordable price [17]; (2) it shows a high hydrophilic character, due to the high presence of aspartic and glutamic acids in its composition [18]; and (3), in combination with a plasticizer (i.e., glycerol), it displays excellent processability

* Corresponding author.
E-mail address: aguerrero@us.es (A. Guerrero).

http://dx.doi.org/10.1016/j.polymertesting.2016.12.024
0142-9418/

properties, allowing the production of different shaped products (e.g. by injection molding) [19].

However, previous studies found in the literature based on soy-protein plastics [18–20] reported water uptake capacities that did not fall within the level required for SAP materials. Correct functionalization of the protein matrix, which would give rise to the presence of new water-solubilizing groups, would improve the water uptake capacity of the material. One of the most common chemical modifications used for proteins is the acylation of the amino acid residues with acid anhydrides [21]. On these grounds, Hwang and Damodaran [16,22] reported that the modification of lysyl residues using ethylenediaminetetraacetic dianhydride (EDTAD) as acylating agent is able to incorporate a large number of carboxylate anions (COO^-) into the soy protein molecule, creating numerous sites for water binding and, consequently, increasing its hydrophilic character. In this research, we propose the use of succinic anhydride (SA) as an alternative acylating agent. Even if SA possesses half the anhydride groups present in EDTAD, its much lower cost (~290 $/lb) compared to EDTAD (~4275 $/lb) would surely play a decisive factor in its eventual industrial application. On this basis, Yoshimura et al. have reported the use of SA in the manufacture of SAP materials made from chitin [23], cotton cellulose [24] and starch [25], whose synthesis involve the use of chemical reagents (e.g. dimethyl sulfoxide, lithium chloride). These SAP materials were solely characterized in terms of their water uptake capacity. Interestingly, the novelty of this research lies in obtaining SAP materials from soy protein and SA as acylating agent, but without the use of those chemical reagents, therefore being a green alternative to non-biodegradable SAP.

Therefore, the main goal of the present work is the production and characterization of natural SAP materials based on an acylated soy protein, obtained through functionalization with SA. Also, broader characterization of the natural SAP plastics processed through injection molding is made through different techniques: dynamic mechanical thermal analysis (DMTA), tensile tests, water uptake capacity measurements and scanning electron microscopy (SEM).

2. Material and methods

2.1. Materials

Soy protein isolate (SPI), under the trade name of SUPRO 500E IP, was supplied by PROANDA (Proveedora Andaluza, S.L., Sevilla, Spain). Its specifications, provided by the supplier, were: max. 6.0% moisture, min. 90.0% protein, max. 1.0% fat, max. 5.0% ash and pH (5% slurry) in the range of 6.9–7.4. Glycerol (GL) and succinic anhydride (SA), from Panreac Química, S.A., were used as protein plasticizer and SPI acylating agent, respectively.

2.1.1. Protein functionalization

The acylation of SPI was performed according to the procedure reported by Zhao et al. [21]. Firstly, a 4 wt% solution of SPI was dispersed in distilled water for 1 h using a magnetic stirrer. Subsequently, the pH of the solution was adjusted to 8 by adding the amount necessary of a 3.0 N NaOH solution. Then, it was modified by the addition of different amounts of SA according to SA/SPI mass ratios of 0.04, 0.08 and 0.12. The pH of the solution was kept between 7.5 and 8.5 adding conveniently 3.0 N NaOH while stirring. After pH was stabilized around 8, the solution was kept stirred for 1 h. Afterwards, pH was decreased to 7.0 by the addition of 3 N HCl to prevent further modification. Finally, the protein solution was dialyzed against deionized water for 48 h to remove impurities and excess reagents, recovering the acylated SPIs through freeze-drying using a Telstar CRYODOS-80 (Telstar, Life Science Solutions, Madrid, Spain).

The acylated SPIs prepared with SA/SPI mass ratio of 0.04, 0.08 and 0.12 will hereinafter be referred to as aSPI-0.04, aSPI-0.08 and aSPI-0.12, respectively.

2.2. Sample preparation

Blends containing 50 wt% protein (unmodified SPI or acylated SPI systems) and 50 wt% GL were properly manufactured by a thermomechanical procedure that consisted of two stages:

a) The ingredients were mixed in a two-blade counter-rotating batch mixer Haake Polylab QC (ThermoHaake, Karlsrube, Germany) at room temperature and 50 rpm for 10 min, under adiabatic conditions. During mixing, only a slight increase in temperature (always lower than 2 °C) was detected, whereas no significant increase in torque was observed, which would exclude any significant contribution of shear-induced cross-linking over the mixing stage. The final pH value of these protein/plasticizer blends was measured by a Crison pH 25 pH meter in combination with a puncture electrode (Crison Instruments S.A., Barcelona, Spain). The values of pH were 8.0 ± 0.5 and 8.4 ± 0.5 for those blends prepared from unmodified SPI and acylated SPIs, respectively. Samples were stored in sealed plastic bags at room temperature for 24 h, prior further processing.
b) The blends were processed after storage for 24 h by lab-scale injection molding using a MiniJet Piston Injection Molding System (ThermoHaake, Karlsrube, Germany) to obtain 60 × 10 × 1 mm rectangular shaped plastic specimens. Based on previous studies searching SPI/GL plastics with optimized water uptake capacity [18], moderate processing conditions were selected. Thus, the temperature, pressure and time in the pre-injection cylinder and in the mold were respectively: 50/120 °C, 500/500 bar and 10/500 s. For the acylated SPIs, the pressure profile selected was 500/250 bar in order to obtain homogeneous plastic specimens.

The plastic materials obtained from unmodified SPI will be referred to as SPI/GL, and those prepared from acylated SPIs as aSPI/GL-0.04, aSPI/GL-0.08 and aSPI/GL-0.12, depending of its SA/SPI mass ratio.

2.3. Characterization

2.3.1. Fourier transform infrared spectroscopy (FTIR)

FTIR spectra of protein samples were recorded on a Jasco FT/IR 4200 spectrometer (Jasco Analytical Instrument, Japan) from finely ground sample (~10 wt %) in KBr pellets. The spectra were obtained in a wavenumber range of 400–4000 cm^{-1} at 4 cm^{-1} resolution in the transmission mode.

2.3.2. Thermo-gravimetric analysis (TGA)

TGA tests were conducted in a Seiko TG/DTA 6200 (Seiko Instruments Inc., Japan). Temperature ramps were carried out using 5–10 mg of protein samples at 10 °C/min, from 30 to 600 °C, under N_2 atmosphere. From these tests, the water loss due to the free and bonded water was calculated in the temperature range from 30 to 150 °C.

2.3.3. Water imbibing capacity (WIC)

The WIC of all protein samples was measured in a Baummann apparatus according to a method modified by Wagner et al. [26]. A glass Buchner funnel equipped with a borosilicate filter (ROBU Glasfilter-Geraete GmbH, Germany) was connected to a horizontal

graduated pipette filled with distilled water and located at the same level as the filter. A 30 mg sample was placed as thin layer on the filter while closing the funnel mouth with a hermetic lid. The amount of liquid water (ml or g) absorbed at room temperature from the pipette was recorded for each material over time until equilibrium was reached, achieving the WIC value.

2.3.4. Dynamic mechanical temperature analysis (DMTA)

DMTA tests were performed on the plastic samples with a RSA3 (TA Instruments, New Castle, USA) in tensile mode using two medium clamps (length: 25 mm; width: 10 mm; thickness: 6 mm) for 60 × 10 × 1 mm rectangular specimens. Temperature sweep tests were conducted at a constant frequency of 1 Hz and strains within the linear viscoelastic region (LVR). Selected temperature ramps were carried out from 0 to 130 °C at 3 °C/min. All the samples were coated with Dow Corning high vacuum grease to minimize water loss.

2.3.5. Static tensile strength measurements

The tensile properties were evaluated at room temperature with a RSA3 (TA Instruments, New Castle, USA) in tensile mode using the above-mentioned clamps for 60 × 10 × 1 mm rectangular specimens. All tensile tests were carried out at constant extension rate of 1 mm/min and the maximum stress (σ_{max}), maximum strain (ε_{max}) and Young's Modulus (E) were obtained.

2.3.6. Water uptake

Water uptake of SAP plastics was determined according to UNE-EN ISO 62:2008 using 20 × 10 × 1 mm specimens immersed in distilled water for 24 h. The water uptake (WU) percentage was calculated as:

$$WU\ (\%) = \frac{m_2 - m_1}{m_1} \times 100 \quad (1)$$

where: m_1 is the initial weight of the specimen immediately weighed after being dried in an oven at 50 °C for 24 h and cooled in a desiccator; and m_2 refers to the weight of the specimen just after 24 h of water immersion.

Moreover, soluble matter loss (SML) was estimated as:

$$SML\ (\%) = \frac{m_1 - m_3}{m_1} \times 100 \quad (2)$$

where: m_3 refers to the final weight of the wet sample after 24 h of drying in an oven at 50 °C and cooled in a desiccator.

2.3.7. Scanning electron microscopy (SEM)

The morphology of freeze-dried plastics after water uptake tests was examined with a scanning electron microscope JEOL JSM 6460 LV (JEOL Solutions for Innovation, USA) with a secondary electron detector at an acceleration voltage of 20 kV. Before any observation, samples cubes of 2–3 mm were cut and treated by Osmium vapor at 1% of concentration for 8 h.

2.3.8. Statistical analysis

In all cases, the data were presented as mean ± standard deviation (SD) of three replicates.

3. Results and discussion

3.1. Characterization of acylated soy protein

The reaction scheme for the SPI functionalization using SA as acylating agent is illustrated in Fig. 1. Acid anhydrides, e.g. SA, do not react selectively with only one type of functional group, but lysine is one of the amino groups most prone to acylation due to its relatively high reactivity and steric availability, if compared to other nucleophilic groups like phenolic and aliphatic hydroxyl groups [21]. Thus, Zhao et al. [21] reported that one carboxylate anion per lysyl residue might be incorporated into soy protein (Fig. 1) following the SPI acylation protocol previously described. This functionalization would impart a polyanionic character to the protein with numerous sites for water binding, thereby increasing its hydrophilic character.

In this context, the FTIR spectra of SA, native SPI and acylated SPIs (Fig. 2) allow to check if the acylation reaction was carried out correctly. As may be observed, all SPIs samples display the same relevant peaks. The absence of the peaks at 1867 and 1783 cm^{-1} in acylated SPI samples confirmed that the reaction products are free of un-reacted SA. The broad peak centred in the range of 3300–3400 cm^{-1} results from the overlapping contributions of the stretching vibrations of both O-H and N-H groups [27]. The characteristic peaks at 1648 and 1543 cm^{-1} are assigned, respectively, to the amide groups (I and II) of the soy protein [27–30]. Amide I corresponds to de C=O stretching vibration (80%) with minor contribution form C-N stretching vibration, and amide II arises from N-H bonding (60%) and C-N stretching vibration (40%) [29,31]. As these bands are strongly influenced by the structure of the protein chain, it can be assumed that they would be significantly modified during the acylation procedure [32]. Table 1 gathers the relative area value between amide II and amide I (A_{1543}/A_{1648}) for SPI samples. It can be observed that A_{1543}/A_{1648} values increase when increasing SA/SPI mass ratio, from 0.36, for native SPI, up to 0.56, for the acylated aSPI-0.12. These results would support the idea that the acylation reaction between $-NH_2$ from the lysyl residue and the anhydride group from SA has taken place to a greater degree for higher SA/SPI values as the occurrence of the reaction would generate new C-N vibrations [29].

On the other hand, the peak at 1405 cm^{-1} related to the symmetric stretching vibrations of COO^- groups [2,21,33] provides valuable information about the extent of acylation. The area of this peak, which is also observed in the native SPI due to the carboxyl group vibrations of aspartic and glutamic acids [21], was normalized with that calculated at 2920 cm^{-1}. This well-defined band, which corresponds to C-H content, represents a good reference for total carbohydrate content, because the number of C-H groups remains constant, irrespective of changes in the SA/SPI mass ratio [27].

It can be observed in Table 1 that the normalized area (A_{1405}/A_{2920}) gradually increases with the SA/SPI mass ratio, achieving a maximum value of 1.31 for SPI-0.12, which would indicate that the acylation reaction takes place to a larger extent.

According to the above-mentioned FTIR results, the incorporation of COO^- groups into soy protein might imply an improvement in its water absorption capacity. Hence, the determination of the water imbibing capacity for protein samples, as well as their thermal analysis, might shed light into this issue.

The kinetics of liquid water absorption, i.e. the amount of water absorbed (WA) by the sample mass unit over time, is displayed in Fig. 3, determining the water imbibing capacity (WIC), expressed as mL absorbed water per g of sample, for all SPI samples once the steady state is reached. The experimental water absorption (WA) value was successfully fitted as a function of time ($r^2 > 0.99$) according to the following equation:

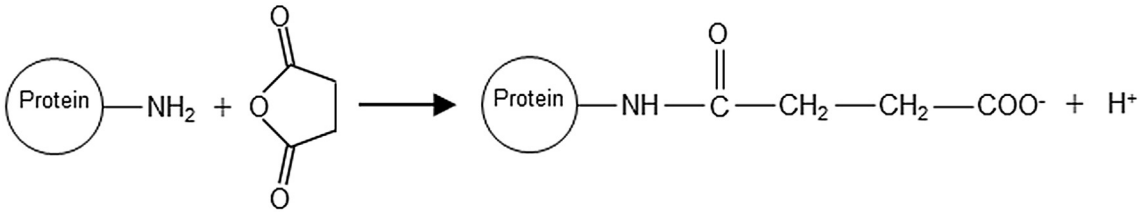

Fig. 1. Reaction scheme for the SPI acylation with SA.

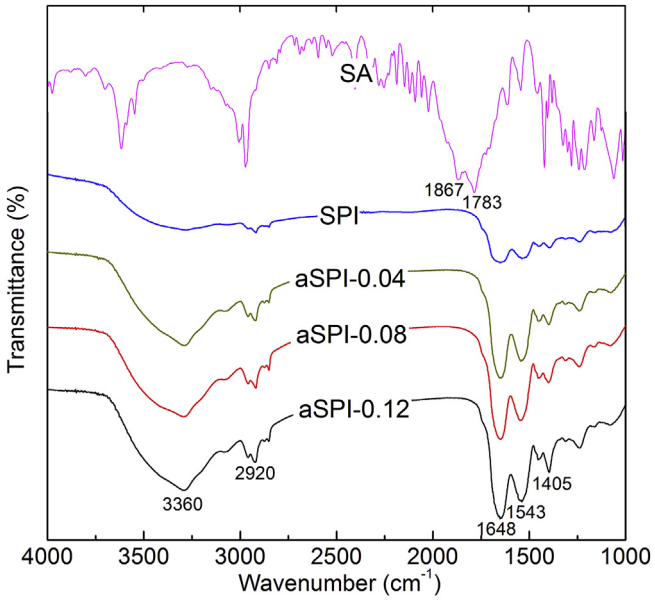

Fig. 2. FTIR spectra of SA, native SPI and acylated SPI samples prepared with different SA/SPI mass ratios.

Table 1
Relative area value between amide II and amide I (A_{1543}/A_{1648}) and normalized area of COO^- groups (A_{1405}/A_{2920}) for native SPI and acylated SPI samples prepared with different SA/SPI mass ratios.

	A_{1543}/A_{1648}	A_{1405}/A_{2920}
SPI	0.36 ± 0.01	0.68 ± 0.01
aSPI-0.04	0.44 ± 0.01	1.03 ± 0.01
aSPI-0.08	0.53 ± 0.01	1.22 ± 0.02
aSPI-0.12	0.56 ± 0.01	1.31 ± 0.03

$$WA = WIC \cdot \left[1 - \frac{1}{1 + \left(\frac{t}{t_{1/2}}\right)^{p}}\right] \quad (3)$$

where WIC is the water imbibing capacity, which is considered as the maximum spontaneous water absorption by the protein powder; $t_{1/2}$ is the time necessary to reach an increase in water absorption of 50%; and 'p' is a parameter related to the slope of the kinetic curve. Table 2 gathers the values of these fitting parameters. It may be observed that a gradual increase in the SA/SPI ratio leads to (a) slower kinetics, characterized by lower 'p' and higher $t_{1/2}$ values, and (b) higher WIC values, which would entail an improvement of the water absorption capacity of SPI when acylated. Thus, the WIC goes from 11.44 mL/g for aSPI-0.04–13.35 mL/g for aSPI-0.12.

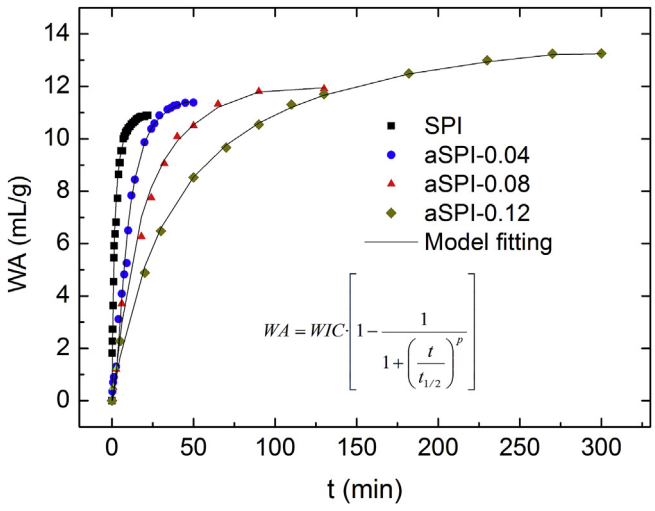

Fig. 3. Water absorption kinetics measured in a Baummann apparatus for native SPI and acylated SPI samples prepared with different SA/SPI mass ratios.

Thermal analysis conducted on the samples would allow us to confirm that result. Fig. 4 shows the TGA curves for unmodified SPI and acylated SPI samples. The TGA profile for all of them are quite coincident, with a first loss of weight related to the release of free and bonded water in the temperature range from 30 to 150 °C, and a second one due to the protein degradation starting at a temperature of about 210 °C [29,32]. If attention is focussed on the first event, the weight remaining at 150 °C significantly increases as the SA/SPI mass ratio increases (Fig. 4), which should be related to its higher hydrophilic character [32]. Therefore, this outcome is in agreement with that obtained from previous WIC measurements, underlining the fact that the chemical modification carried out results in acylated SPI samples with improved hydrophilic properties and, presumably, higher bonded water when compared to the original native protein.

3.2. Characterization of natural superabsorbent plastics

Once the acylated proteins were characterized in terms of the FTIR, WIC, and TGA tests, they were blended thoroughly with a plasticizer resulting in the corresponding protein/glycerol (50/50 wt%) blends. These blends were processed, after storage for 24 h, by injection molding to obtain plastic specimens.

Fig. 5 shows the elastic (E′) and loss (E″) moduli (Fig. 5A) and the loss tangent (tan δ) (Fig. 5B) from DMTA temperature sweep tests for the system prepared from the unacylated protein used as a reference (SPI-GL) and the acylated plastic samples prepared with different SA/SPI mass ratio values. As may be observed in Fig. 5A, they all present qualitatively similar DMTA curves, with a predominantly elastic character, E′ being higher than E″ over the range of temperature values studied. As the temperature rises, both

Table 2
WIC values and fitting parameters ($t_{1/2}$ and 'p') corresponding to Equation (3) for native SPI and acylated SPI samples prepared with different SA/SPI mass ratios.

	WIC (mL/g)	$t_{1/2}$(min)	p
SPI	10.92 ± 0.10	1.37 ± 1.45	1.94 ± 0.11
aSPI-0.04	11.44 ± 0.11	8.60 ± 1.75	1.83 ± 0.16
aSPI-0.08	12.03 ± 0.25	16.35 ± 4.39	1.22 ± 0.12
aSPI-0.12	13.35 ± 0.15	38.03 ± 6.76	1.02 ± 0.10

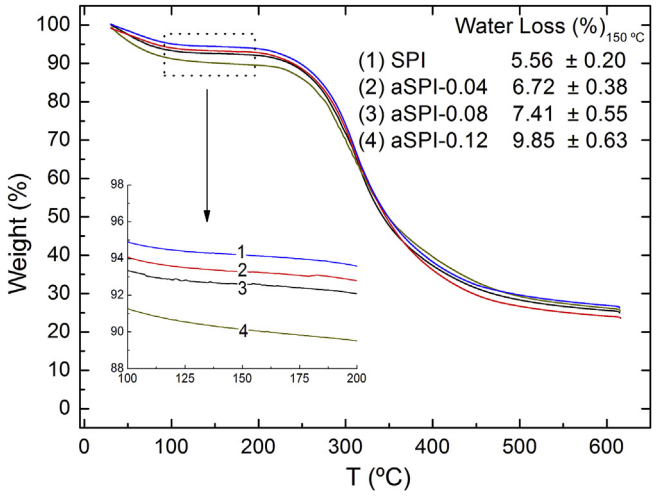

Fig. 4. TGA curves for native SPI and acylated SPI samples prepared with different SA/SPI mass ratios.

moduli decrease toward a plateau region, which is observed above 80 °C. Subsequently, this plateau is followed by a decrease in both moduli, being more pronounced for E″, which proves that the plastics thermos-setting, caused by protein denaturation, mainly occurs during the previous compression-mould process at 120 °C [15]. On the other hand, acylated SPI samples produces plastics with lower viscoelastic moduli (E′ and E″) compared to the reference plastic. This softening in the acylated plastics observed in DMTA tests was greater as the SA/SPI mass ratio increases. In contrast, as observed in Fig. 5B, acylation of SPI leads to a significant modification of the tan δ profile shown for the reference sample. Thus, unacylated SPI-based plastic shows two peaks in tan δ at 48 °C and 92 °C, the first of which has been previously found for injection-molded soy/glycerol plastic samples [19,20]. However, no second peak at high temperature was previously detected for such samples, which might be associated to the higher injection pressure applied in those cases as compared to the one used in the present study.

Plastic samples molded with acylated SPI show the same two peaks, although the first one is forming a shoulder. A displacement of both peaks towards a slightly higher temperature may be also observed. However, the most remarkable effect that takes place when using acylated SPI used instead of native SPI peak is the development of a new peak at low temperature. In fact, this peak seems to be sheltered in the mean peak of the reference system and progressively shifts towards lower temperature as the extent of acylation reaction increases.

Several authors have previously reported occurrence of different glass transition temperatures from DMTA results of soy protein/glycerol films having similar ratios (a low-temperature transition at about −60 °C and a high-temperature transition in the range of 50–75 °C). These transitions have been explained as the result of local nonhomogeneous regions of glycerol/soy protein with some

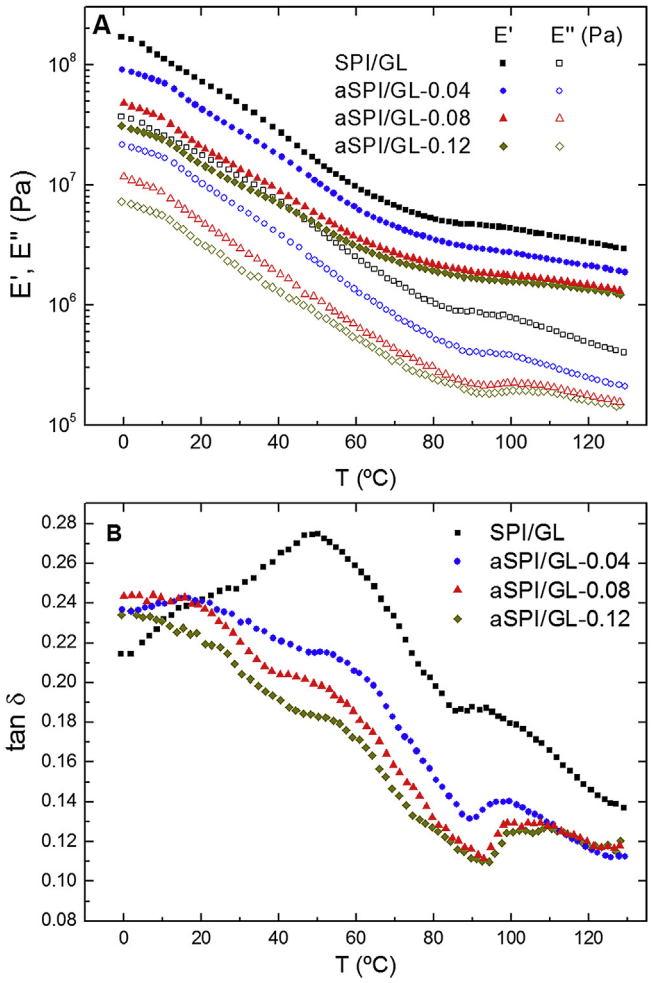

Fig. 5. Linear viscoelastic response at constant frequency (1 Hz) from DMTA in tensile mode for the reference and acylated plastics processed through injection molding, as a function of temperature: (A) E′ and E″; (B) tan δ.

regions dominated by the plasticizer and others by protein. Thus, if sufficient protein were to diffuse into the glycerol phase, it would have an elevating effect on the T_g of glycerol (reported to be at ca. −93 °C). On the other hand, the diffusion of glycerol into the protein phase would depress the T_g of soy protein (which would lie in the range of 150–200 °C). Both effects can lead to remarkable changes in their respective T_g values [19,20,34–36]. A third glass transition, taking place in the high-temperature regime (ca. 120–150 °C), was reported by Ogale et al. [37]. These authors attributed this high-temperature transition to local regions of more highly concentrated protein likely associated with a loss of plasticizer. In the present case, tan δ results indicate that acylated SPI samples yield a redistribution of the different plasticized protein fractions resulting in a higher contribution of the glycerol-rich fractions (i.e. showing lower glass transition temperature). These results suggest that the relative proportion of protein plasticized by glycerol increase with acylation.

The results obtained from uniaxial strength measurements for the resulting plastic samples are shown in Fig. 6. In Fig. 6A, the stress-strain curves for the reference and acylated plastics are displayed. All the curves exhibit initial linear elastic behavior of high constant stress–strain slope yielding high values for the Young's Modulus (E), followed by a plastic deformation stage with a continuous decrease in the stress–strain slope after the elastic

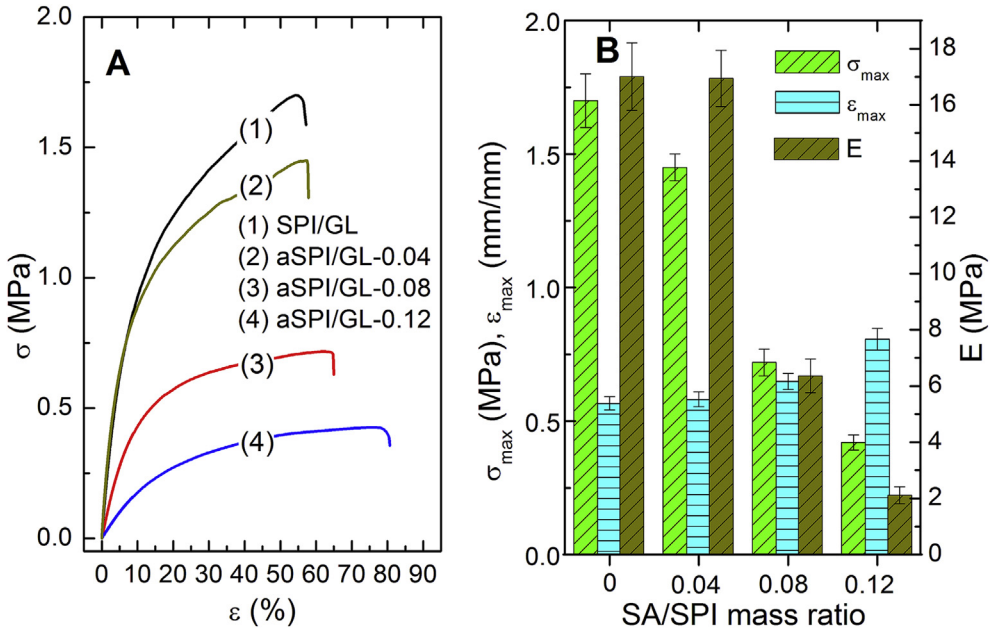

Fig. 6. Results from tensile strength measurements for the reference and acylated plastics processed through injection molding: (A) stress versus strain curves; and (B) parameters from tensile strength measurements: Maximum stress (σ_{max}), maximum strain (ε_{max}) and Young's Modulus (E).

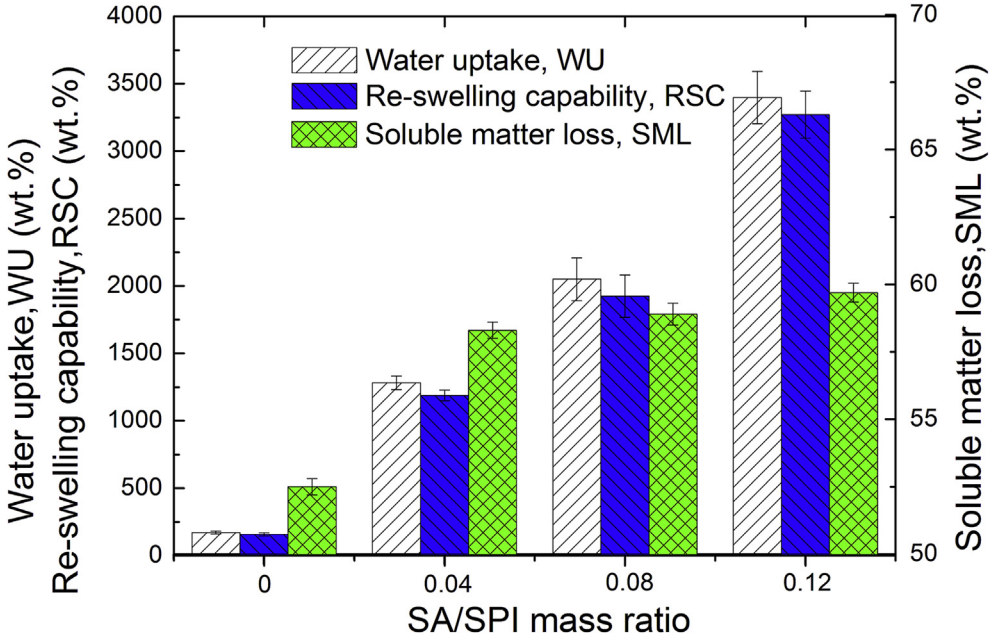

Fig. 7. Water uptake capacity results after immersion for 24 h and loss of soluble matter for the reference and acylated plastics processed through injection molding.

limit. A second constant slope is reached at the end of this plastic deformation stage. All the curves eventually reach a maximum value for the stress (σ_{max}) and the strain (ε_{max}), which is immediately followed by a sudden decrease in stress that corresponds to the rupture of the sample. Fig. 6B shows the values of three representative parameters (E, σ_{max} and ε_{max}) from these tensile tests performed on plastic specimens, as a function of the SA/SPI mass ratio. Both σ_{max} and E show a progressive decrease with increasing SA/SPI mass ratio, with a drop of 75% and 88% in both values, respectively, for the aSPI/GL-0.12 plastic when compared to the reference sample, which is consistent with its poorer elastic response found from the DMTA. On the contrary, ε_{max} undergoes an increase when compared to the reference plastic up to 3, 15 and 43% as SA/SPI mass ratio gradually increases (0.04, 0.08, 0.12, respectively). This effect is consistent with the higher plasticizing efficiency inferred from tan δ (Fig. 5B) for aSPI-based samples. Both effects (i.e., decrease in σ_{max} and E, and increase in ε_{max}) are more significant for acylated plastics prepared from highly modified proteins, with SA/SPI mass ratios higher than 0.04.

Therefore, it may be stated that the SPI chemical modification by acylation produces plastics less fragile than the reference sample, which becomes more noticeable by increasing SA/SPI mass ratio.

Fig. 7 shows the results from the water uptake measurements obtained after immersion of plastic samples for 24 h, as well as

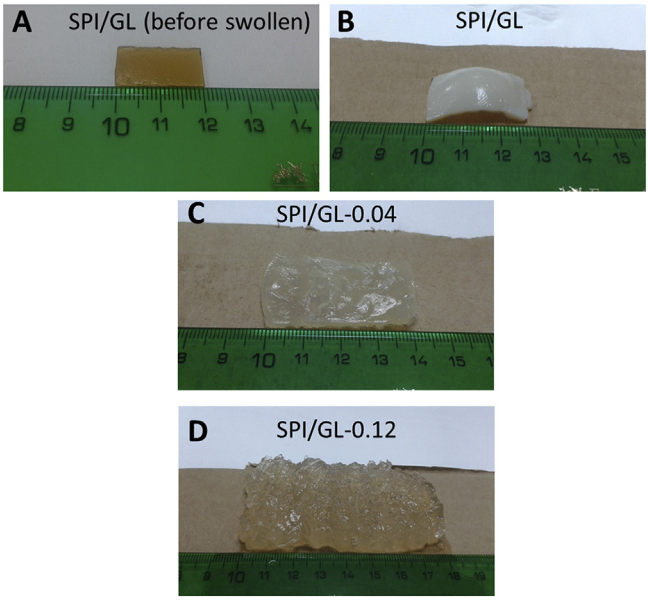

Fig. 8. Images of different plastic samples: (A) Reference sample plastic before water immersion for 24 h; (B), Reference sample after water uptake; Acylated plastics after water uptake for a SA/SPI mass ratio of (C) 0.04 and (D) 0.12.

their corresponding water-soluble matter loss, as a function of SA/SPI mass ratio. As it can be deduced, water uptake (WU) capacity is much higher for acylated plastics compared to the relatively poor value obtained for the reference sample. In addition, a gradual growth in water uptake is also observed as SA/SPI mass ratio rose. Thus, water uptake values of the acylated samples are 655, 1106 and 1904% higher in comparison to the plastic used as reference when the SA/SPI mass ratio is 0.04, 0.08 and 0.12, respectively. These water uptakes values correspond to 12.8, 20.5 and 34.0 times their own dry weight and, therefore, all acylated plastics achieve the level required to be considered as superabsorbent materials [1–3]. The differences in water uptake capacity of plastics are clearly illustrated by comparing the photographs included in Fig. 8. All acylated plastic samples before water immersion present similar physical appearance to that of the reference plastic (Fig. 8A). This non-acylated sample is moderately swollen by water after 24 h (Fig. 8B) when compared to acylated samples (Fig. 8C and D for SA/SPI mass ratio of 0.04 and 0.12, respectively). Thus, it can be clearly seen that the wet acylated samples are larger in size, and also more transparent, when they are prepared from SPI with higher SA/SPI mass ratio. Regarding the water-soluble loss matter (SML), reference plastic shows a value of 52.5%, and all the acylated systems exhibited values that are slightly higher, ranging from 58.3, for aSPI/GL-0.04, to 59.7%, for aSPI/GL-0.12 (Fig. 7). The result for the reference sample suggests that its loss of soluble matter corresponds mainly to the glycerol initially contained in the plastic (~50%), which is known to be highly hydrophilic, and to a minor extent to some protein that is not strongly associated to the network structure; whereas, the extra-loss matter observed for acylated plastics, could be caused by the higher hydrophilic character observed for SPI acylated samples that would favour its solubilization compared to the unacylated sample (Figs. 3 and 4).

On the other hand, the wet plastics were lyophilized and again subjected to water immersion for 24 h (named as re-swelling capability, RSC). Interestingly, no significant modification in water uptake may be found in Fig. 7 after re-swelling of superabsorbent plastics. In addition to that, no water-soluble loss matter was observed for the acylated plastics after the second water immersion, as no glycerol or soluble protein is left in the plastic material after the first immersion. These results are particularly relevant from a practical point of view, since they would imply that SPI superabsorbent materials could be re-used at least twice without losing their water uptake capacity.

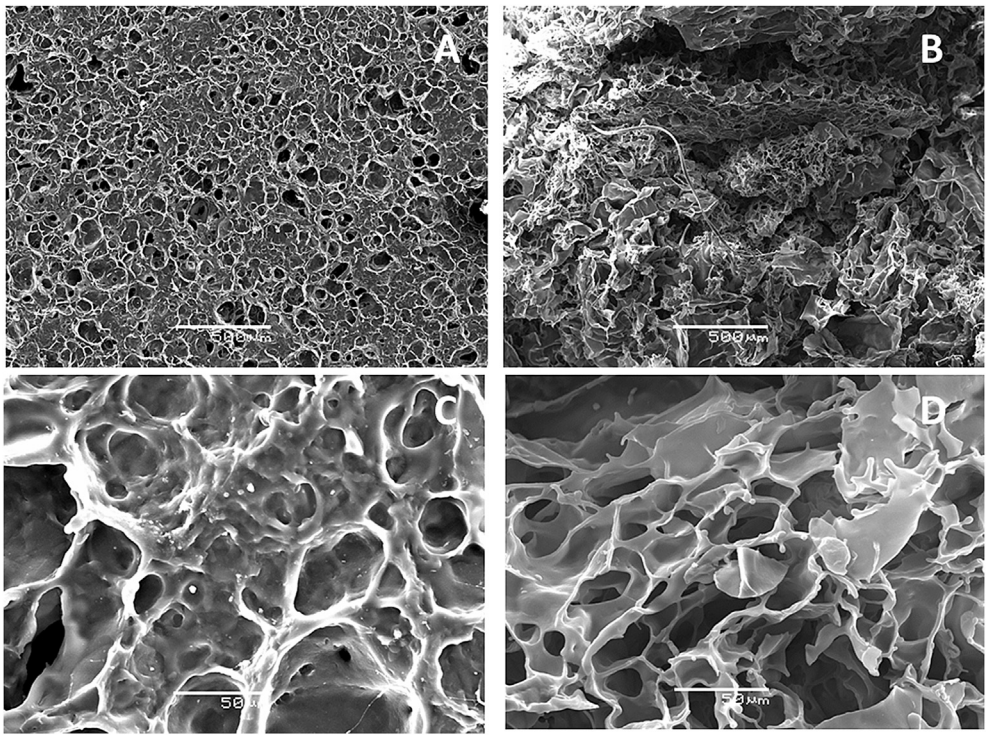

Fig. 9. SEM micrographs of reference (A and C) and SPI/GL-0.12 (B and D) freeze dried plastics, processed through injection molding, after water immersion.

Finally, the morphology of freeze-dried plastics after water immersion for 24 h, were observed by SEM at two different magnifications for the reference and acylated aSPI/GL-0.12 systems (Fig. 9). As may be seen, even if both samples present a good three-dimensional network structure, important differences should be highlighted. On the one hand, the reference system (Fig. 9A and C) exhibits many pores with diameter lower than ca. 100 μm distributed uniformly on the surface of the materials. This porous region was probably the site where the water permeation occurred and the water binding takes places [1,38]. Thus, its matrix displays an arrangement with closed pores which clearly difficult the water permeation/binding. On the other hand, SEM micrographs revealed that a highly open porous structure, with pores being larger and irregular in shape, is noticed on the acylated SPI sample (Fig. 9B and D). These SEM images for the acylated sample, which resembles the images obtained from hydrogels such as those prepared using collagen [39], confers the possibility to absorb large amounts of water through these hollow spaces.

4. Concluding remarks

With the aim of developing natural-based superabsorbent polymers (SAP) plastics processed through injection molding, the acylation of soy protein (SPI) with succinic anhydride (SA), using different SA/SPI mass ratio values, was evaluated.

The FTIR results performed on acylated SPI samples showed that carboxylate anions are incorporated into the SPI molecule due to the reaction between $-NH_2$ of lysyl residue and the anhydride group of SA. Thus, the protein hydrophilic character is clearly enhanced, as proven from the determination of the water imbibing capacity (WIC). In this sense, the WIC goes up to 22.3% of the value corresponding to native SPI when the SA/SPI mass ratio was 0.12. As a consequence, the water uptake capacity of plastic samples is strongly enhanced for acylated plastics (with values of 1282, 2050 and 3398 wt% for SA/SPI mass ratio of 0.04, 0.08 and 0.12, respectively) compared to the moderate value obtained for the reference sample (170 wt%). In this sense, SEM images corroborated that larger porous region were developed in the acylated plastic. Thus, all acylated natural-based plastics achieve the water uptake level required to be considered as superabsorbent materials. Interestingly, it was proved that these materials could be re-used at least twice without losing their water uptake capacity. In addition to that, freeze-dried acylated samples (after 1 freeze-drying cycle) may be regarded as highly promising candidates for applications in which maintaining the dimensional stability during service is not crucial (e.g. in agriculture and horticulture). As for their thermo-mechanical properties, acylated plastics showing a higher tendency to the segregation of GL-rich and aSPI-rich fractions and lower viscoelastic moduli, as well as a higher extensibility, compared to the reference plastic, were deduced from DMTA and static tensile strength measurements, respectively.

Acknowledgements

This work is part of a research project sponsored by “Ministerio de Economía y Competitividad” from Spanish Government (Ref. CTQ2015-71164-P). The authors gratefully acknowledge their financial support. The authors also acknowledge to CIITUS (Universidad de Sevilla) for providing full access and assistance to the SEM of the Microscopy Service.

References

[1] W. Shi, M.J. Dumont, E.B. Ly, Synthesis and properties of canola protein-based superabsorbent hydrogels, Eur. Polym. J. 54 (2014) 172.
[2] M. Irani, H. Ismail, Z. Ahmad, Preparation and properties of linear low-density polyethylene-g-poly (acrylic acid)/organo-montmorillonite superabsorbent hydrogel composites, Polym. Test. 32 (3) (2013) 502.
[3] M.J. Ramazani-Harandi, M.J. Zohuriann-Mehr, A.A. Yousefi, A. Ershad-Langroudi, K. Kabiri, Rheological determination of the swollen gel strength of superabsorbent polymer hydrogels, Polym. Test. 25 (4) (2006) 470.
[4] F. Ullah, M.B.H. Othman, F. Javed, Z. Ahmad, H.M. Akil, Classification, processing and application of hydrogels: a review, Mat. Sci. Eng. C-Mater 57 (2015) 414.
[5] M.R. Guilherme, F.A. Aouada, A.R. Fajardo, A.F. Martins, A.T. Paulino, M.F.T. Davi, A.F. Rubira, E.C. Muniz, Superabsorbent hydrogels based on polysaccharides for application in agriculture as soil conditioner and nutrient carrier: a review, Eur. Polym. J. 72 (2015) 365.
[6] K. Kosemund, H. Schlatter, J.L. Ochsenhirt, E.L. Krause, D.S. Marsman, G.N. Erasala, Safety evaluation of superabsorbent baby diapers, Regul. Toxicol. Pharm. 53 (2) (2009) 81.
[7] M.J. Zohuriaan-Mehr, K. Kabiri, Superabsorbent polymer materials: a review, Iran. Polym. J. 17 (6) (2008) 451.
[8] A. Jamshidi, F. Ahmad Khan Beigi, K. Kabiri, M.J. Zohuriann-Mehr, Optimized HPLC determination of residual monomer in hygienic SAP hydrogels, Polym. Test. 24 (7) (2005) 825.
[9] H. Kubota, S. Kuwabara, Cellulosic absorbents for water synthesized by grafting of hydrophilic vinyl monomers on carboxymethyl cellulose, J. Appl. Polym. Sci. 64 (11) (1997) 2259.
[10] J.H. Wu, J.M. Lin, M. Zhou, C.R. Wei, Synthesis and properties of starch-graft-polyacrylamide/clay superabsorbent composite, Macromol. Rapid Comm. 21 (15) (2000) 1032.
[11] A. Pourjavadi, A.M. Harzandi, H. Hosseinzadeh, Modified carrageenan 3. Synthesis of a novel polysaccharide-based superabsorbent hydrogel via graft copolymerization of acrylic acid onto kappa-carrageenan in air, Eur. Polym. J. 40 (7) (2004) 1363.
[12] K. Burugapalli, D. Bhatia, V. Koul, V. Choudhary, Interpenetrating polymer networks based on poly(acrylic acid) and gelatin. I: swelling and thermal behaviour, J. Appl. Polym. Sci. 82 (1) (2001) 217.
[13] M. Teodorescu, A. Lungu, P.O. Stanescu, C. Neamtu, Preparation and properties of novel slow-release NPK agrochemical formulations based on Poly(acrylic acid) hydrogels and liquid fertilizers, Ind. Eng. Chem. Res. 48 (14) (2009) 6527.
[14] M.A. Hubbe, A. Ayoub, J.S. Daystar, R.A. Venditti, J.J. Pawlak, Enhanced absorbent products incorporation cellulose and its derivatives: a review, Bioresources 8 (4) (2013) 6556.
[15] M.L. López-Castejón, C. Bengoechea, M. García-Morales, I. Martínez, Effect of plasticizer and storage conditions on thermomechanical properties of albumen/tragacanth based bioplastics, Food Bioprod. Process 95 (2015) 264.
[16] D.C. Hwang, S. Damodaran, Chemical modification strategies for synthesis of protein-based hydrogel, J. Agr. Food Chem. 44 (3) (1996) 751.
[17] H.F. Tian, W.Q. Wu, G.P. Guo, B. Gaolun, Q.Q. Jia, A.M. Xiang, Microstructure and properties of glycerol plasticized soy protein plastics containing castor oil, J. Food Eng. 109 (3) (2012) 496.
[18] L. Fernández-Espada, C. Bengoechea, F. Cordobés, A. Guerrero, Protein/glycerol blends and injection-molded bioplastic matrices: soybean versus egg albumen, J. Appl. Polym. Sci. 133 (6) (2016) 42980.
[19] M. Félix, J.E. Martín-Alfonso, A. Romero, A. Guerrero, Development of albumen/soy biobased plastic materials processed by injection molding, J. Food Eng. 125 (2014) 7.
[20] L. Fernández-Espada, C. Bengoechea, F. Cordobés, A. Guerrero, Thermo-mechanical properties and water uptake capacity of soy protein-based bioplastics processed by injection molding, J. Appl. Polym. Sci. 133 (24) (2016) 43524.
[21] Y. Zhao, C.Y. Ma, S.N. Yuen, D.L. Phillips, Study of succinylated food proteins by Raman spectroscopy, J. Agr. Food Chem. 52 (7) (2004) 1815.
[22] D.C. Hwang, S. Damodaran, Equilibrium swelling properties of a novel ethylenediaminetetraacetic dianhydride (EDTAD)-modified soy protein hydrogel, J. Appl. Polym. Sci. 62 (8) (1996) 1285.
[23] T. Yoshimura, I. Uchikoshi, Y. Yoshiura, R. Fujioka, Synthesis and characterization of novel biodegradable superabsorbent hydrogels based on chitin and succinic anhydride, Carbohyd Polym. 61 (3) (2005) 322.
[24] T. Yoshimura, K. Matsuo, R. Fujioka, Novel biodegradable superabsorbent hydrogels derived from cotton cellulose and Succinic anhydride: synthesis and characterization, J. Appl. Polym. Sci. 99 (6) (2006) 3251.
[25] T. Yoshimura, R. Yoshimura, C. Seki, R. Fujioka, Synthesis and characterization of biodegradable hydrogels based on starch and succinic anhydride, Carbohyd Polym. 64 (2) (2006) 345.
[26] J.R. Wagner, D.A. Sorgentini, M.C. Anon, Thermal end electrophoretic behavior, hydrophobicity, and some functional properties of acid-treated soy isolates, J. Agr. Food Chem. 44 (7) (1996) 1881.
[27] J.C. Spada, L.D.F. Marczak, I.C. Tessaro, N.S.M. Cardozo, Interactions between soy protein from water-soluble soy extract and polysaccharides in solutions with polydextrose, Carbohyd Polym. 134 (2015) 119.
[28] L. Wang, M. Xiao, S. Dai, J. Song, X. Ni, Y. Fang, H. Corke, F. Jiang, Interactions between carboxymethyl konjac glucomannan and soy protein isolate in blended films, Carbohyd Polym. 101 (2014) 136.
[29] H. Liu, X.S. Sun, Improved water resistance in undecylenic acid (UA)-modified soy protein isolate (SPI)-based adhesives, Ind. Crop Prod. 74 (2015) 577.
[30] S. Rolere, S. Liengprayoon, L. Vaysse, J. Sainte-Beuve, F. Bonfils, Investigating natural rubber composition with Fourier Transform Infrared (FT-IR)

spectroscopy: a rapid and non-destructive method to determine both protein and lipid contents simultaneously, Polym. Test. 43 (2015) 83.
[31] A.A. Bunaciu, S. Fleschin, H.Y. Aboul-Enein, Infrared microspectroscopy applications – review, Curr. Anal. Chem. 10 (1) (2014) 132.
[32] H. Winkler, W. Vorwerg, M. Schmid, Synthesis of hydrophobic whey protein isolate by acylation with fatty acids, Eur. Polym. J. 62 (2015) 10.
[33] A.M. Senna, K.M. Novack, V.R. Botaro, Synthesis and characterization of hydrogels from cellulose acetate by esterification crosslinking with EDTA dianhydride, Carbohyd Polym. 114 (2014) 260.
[34] M.T. Kalichevsky, E.M. Jaroszkiewicz, J.M.V. Blanshard, Glass transition of gluten. 1: gluten and gluten-sugar mixtures, Int. J. Biol. Macromol. 14 (5) (1992) 257.
[35] P. Chen, L. Zhang, New evidences of glass transitions and microstructures of soy protein plasticized with glycerol, Macromol. Biosci. 5 (3) (2005) 237.
[36] P. Chen, L. Zhang, F. Cao, Effects of moisture on glass transition and microstructure of glycerol-plasticized soy protein, Macromol. Biosci. 5 (9) (2005) 872.
[37] A.A Ogale, P. Cunningham, P.L Dawson, J.C Acton, Viscoelastic, thermal, and microstructure characterization of soy protein isolate films, J. Food Sci. 65 (4) 672.
[38] A. Pourjavadi, M. Kurdtabar, Collagen-based highly porous hydrogel without any porogen: synthesis and characteristics, Eur. Polym. J. 43 (3) (2007) 877.
[39] S. Potorac, M. Popa, V. Maier, G. Lisa, L. Verestiuc, New hydrogels based on maleilated collagen with potential applications in tissue engineering, Mat. Sci. Eng. C-Mater 32 (2) (2012) 236.